Separation and Purification Technology 75 (2010) 198–203

Robust synthesis and performance of a titania-based ultrafiltration membrane with photocatalytic properties

Lahcène Djafer[a,b], André Ayral[a,*], Abdallah Ouagued[b]

[a] Institut Européen des Membranes, CNRS-ENSCM-UM2, cc047, Université Montpellier 2, Place Eugène Bataillon, F-34095 Montpellier cedex 5, France
[b] Laboratoire Eau – Environnement, Université Hassiba Ben Bouali, BP 151, 02000 Chlef, Algeria

ARTICLE INFO

Article history:
Received 16 November 2009
Received in revised form 19 April 2010
Accepted 3 August 2010

Keywords:
Titania sol
Multifunctional membrane
Separation
Photocatalysis

ABSTRACT

Direct coupling of separation and photocatalytic degradation by using photocatalytic membrane is an attractive way to solve problems like membrane fouling by adsorbed organic macromolecules or elimination of small organic molecules which cannot be efficiently stopped by a membrane.

A simple and robust synthesis route to a photocatalytically active titania membrane is here developed from a commercial titania hydrosol and commercial alumina supports. Reproducible defect-free layers with a thickness of about 3 μm are prepared. The membrane performance in term of separation and photocatalytic activity are investigated. The pure water permeance is ~150 L h^{-1} m^{-2} bar^{-1} and the measured molecular weight cut-off is around ~50 kDa corresponding to an ultrafiltration membrane. The photocatalytic efficiency is tested by photo-oxidation under UV irradiation of a reference organic dye (methylene blue) for comparison with reference titania photocatalysts, and also with phenol as typical organic pollutant in water. The measured values of quantity of destroyed organic molecules per units of time and of membrane surface area are in the range 0.8–3.8 × 10^{-8} mol s^{-1} m^{-2}.

1. Introduction

Membrane technology takes an increasing role in water treatment processes for both the production of tap water and the treatment and recycling of waste water. On the other hand, photocatalysis is an advanced oxidation technique with promising opportunities of applications in the treatment of polluted air [1] or water [2]. Hybrid photocatalysis-membranes systems with different possible configurations are intensively investigated since few years [3–6]. Direct coupling of separation and photocatalytic degradation by using photocatalytic membranes [7–11] is an attractive way to solve some membrane limitations. A first example is related to membrane fouling by adsorbed organic macromolecules which could be overcame by photodegradation. A second example deals with small organics like phenol which are not easy stopped by membrane filtration. They could be mineralized as they go across the membrane which would act in that case as a very efficient photocatalytic contactor.

Titania is the reference material in term of photocatalytic efficiency under UV irradiation, with already well-established technological applications [12]. It also exhibits a very good chemical stability as ceramic membrane. The two main crystalline forms, anatase and rutile, are both photoactive. The gap of anatase is equal to 3.23 eV (384 nm) whereas the gap of rutile is equal to 3.02 eV (411 nm) [13]. The crystalline form anatase is known to be the most photoactive [14,15]. However mixtures of anatase and rutile phases like for instance the standard powder P25 (from Evonik; anatase: 80 wt%, rutile: 20 wt%) enable to limit the recombination of charges due to the lower gap of rutile but their photocatylitic activity strongly depends on the compounds to be degraded [16–19].

This study deals with the development of a simple and robust synthesis of a titania-based ultrafiltration (UF) membrane from a commercial titania hydrosol deposited on commercial macroporous alumina supports. Its performance in term of separation (pure water permeance, molecular weight cut-off) and photocatalytic activity are investigated. The photocatalytic efficiency is tested by photo-oxidation under UV irradiation of a reference organic dye (methylene blue) for comparison with reference titania photocatalysts, and also with phenol as typical organic pollutant in water.

2. Experimental

2.1. Material syntheses

From preliminary experiments with commercially available basic and acidic titania hydrosols [20], the selected starting sol was the basic hydrosol S5-300B, purchased from Mille-

* Corresponding author. Tel.: +33 4 67 14 91 43; fax: +33 4 67 14 91 19.
E-mail address: andre.ayral@iemm.univ-montp2.fr (A. Ayral).

1383-5866/$ – see front matter © 2010 Elsevier B.V. All rights reserved.
doi:10.1016/j.seppur.2010.08.001

nium Inorganic Chemicals France. Its main characteristics are: TiO_2 = 17.5 wt%, pH 11.5, specific surface area >250 $m^2 g^{-1}$, crystalline form: anatase, particle size (from TEM) = 30–60 nm, crystallite size (from XRD) = 5–10 nm. Based on the particle size, the high specific surface area value can be explained by an important contribution of the interparticle porosity to the total surface area.

One volume of this starting sol was first mixed with 9 volumes of ammonia aqueous solution with pH 11.5. Hydroxyethyl cellulose was used as organic binder (HEC, ref. no. 54290 from Fluka). An aqueous solution with HEC = 5 wt% was separately prepared. It was then poured under stirring in the diluted titania sol with a volume ratio 1:7.5. In order to control the membrane thickness, this mixture was finally two-fold diluted using the same ammonia aqueous solution (pH 11.5) as for the first dilution step.

A commercial titania powder P25 (anatase: 80 wt%; rutile: 20 wt%, specific surface area = 50 ± 15 $m^2 g^{-1}$, from Evonik) was used as standard powder for photocatalysis to be compared with powder B resulting from drying and calcination of the formulated titania sol. It must be here noted that powder P25 consists of nanoparticles aggregates and, even after efficient dispersion in water, aggregates larger than a few hundred nanometers remain in the suspension [21]. As consequence, the use of this commercial powder as starting material for the preparation of ultrafiltration membranes is problematic.

2.2. Coatings and membranes

Membranes were prepared by slip-casting on asymmetric tubular alumina supports (length 200 mm; internal diameter 7 mm; 200 nm pore-sized top layer, from Pall Exekia). Additional samples were prepared by dip-coating on alumina disks (diameter 47 mm, thickness 1 mm, 200 nm pore-sized top layer, from Inocermic). The contact time was 30 seconds and the emptying/withdrawal rate was 2 cm min^{-1}. Equivalent powder B was obtained by drying the formulated sol in large beakers.

All the samples were dried at room temperature for 1 day. A thermal treatment was then carried out for removal of the organic binder and mechanical strengthening of the deposited layers. It was consisted of two dwells of 24 h at 250 and 450 °C, respectively, with a heating rate of 0.5 °C min^{-1} and a natural cooling rate at the end of the second dwell. After calcination, the equivalent powder B was manually ground using an agate mortar.

2.3. Characterization

Layer morphology observations were made by scanning electron microscopy (SEM). The porous texture of powder B was characterized by nitrogen adsorption–desorption isotherms at 77 K using a volumetric apparatus. The BJH method [22] was applied for determination of the mean mesopore equivalent diameter, assuming cylindrical pores. The same apparatus was used to determine the specific surface area of powder B by the BET method [23].

The water permeability measurements were performed on the tubular membranes with a home-made tangential filtration device. The measurements were carried out for transmembrane pressures in a range between 1 and 6 bar. The circulation speed of water along the membrane was fixed at 2.7 m s^{-1} by means of a circulation pump.

The cut-off of the membrane was determined using an aqueous solution containing a mixture of three Dextran®: 1.25 g L^{-1} of D-92600 (average MW = 10,200); 0.50 g L^{-1} of D-4133 (average MW = 38,900); 0.50 g L^{-1} of D-1390 (average MW = 72,600), all purchased from Sigma. The transmembrane pressure was fixed at 2 bar. The solute contents in the permeate were measured from analyses by size exclusion chromatography coupled with an interferometric refractometer as detector.

The photocatalytic activity of powder B was evaluated by analyzing the photodegradation of an organic dye, Methylene Blue (MB) or of phenol, in aqueous solution. MB is a reference molecule frequently used to evaluate the activity of photocatalysts. Phenol is a typical pollutant in water. Oxygen required for the catalytic photo-oxidation of these organic molecules was provided by dissolution from the air surrounding the used aqueous solutions. 10 mg of powder B or of reference powder P25 were placed without stirring in a Petri box containing 10 mL of different aqueous solutions: 5 mg L^{-1} (∼2×10^{-5} mol L^{-1}) of MB or 10 mg L^{-1} (∼10^{-4} mol L^{-1}) of phenol or 100 mg L^{-1} (∼10^{-3} mol L^{-1}) of phenol. The used UV lamp had a polychromatic spectrum and an irradiance of 35 W m^{-2} (measured with the UV radiometer at the bottom level of the Petri box). This UV irradiation is corresponding to ∼1×10^{-4} mol of photon s^{-1} m^{-2}. The evolution of the MB concentration versus irradiation time was performed by colorimetric measurements at λ = 664 nm ($\varepsilon_{MB} = 8 \times 10^4$ cm^{-1} L mol^{-1}). In the case of phenol, the best results in term of accuracy were obtained with a calibration curve and solution measurements established from the areas of the UV spectra in the range [200–400 nm].

Experiments on photocatalytic membranes were mainly carried out with a simplified experimental diffusion set-up consisted of two glass tanks separated with the flat membrane (Fig. 1a) and following a previously used procedure [9]. The volume of liquid in the feed and reception tanks, V, was equal to 75 cm^3 and the membrane area, A, was equal to 11 cm^2. The feed tank contained the aqueous solution of MB with an initial concentration of 10^{-4} mol L^{-1} or of phenol with an initial concentration of 10^{-3} mol L^{-1}. The reception tank was initially filled with pure water. After a first stage with a contact time of 1 day in order to saturate the membrane surface with adsorbed organic molecules, the feed and reception tanks were replaced by fresh aqueous solution and pure water, respectively. This operation corresponded to the starting time ($t = 0$) for the organic solute diffusion experiment. During several ranges of times, alternated periods of 1 h without UV irradiation (increase of organic concentration in the reception tank due to the concentration gradient between both membrane sides) and of 1 h under UV irradiation (usually, decrease of the organic solute concentration in the reception tank due to photodegradation in spite of continuous diffusion transport). The UV irradiation was applied on the titania top layer placed in contact with the reception solution. The used UV lamp was the same as for the measurement on powders with the same measured UV irradiation value. The feed and reception tanks were gently stirred with magnetic bars.

Additional experiments were performed in dynamic conditions using a modified configuration (Fig. 1b). The feed tank contained an aqueous solution of MB with a concentration of 2×10^{-7} mol L^{-1} and the applied transmembrane pressure ΔP was equal to 1.2 bar. UV irradiation was continuously maintained during the experiment.

3. Results and discussion

3.1. Membrane preparation and morphology

An important objective of this study was the development of simple and easily repeatable preparation process. The strategy was to use a commercially available hydrosol of anatase with a high oxide content as titania source. In the optimized procedure, this sol is only diluted with an aqueous ammonia solution exhibiting the same pH as the starting sol. The choice of ammonia rather than soda or potassium hydroxide is due to the fact than the presence of alkaline ions in the titania network can disturbed its photocatalytic activity. Finally, the used organic binder, i.e. HEC, is rather cheap and commonly used as additive in conventional ceramic processes.

Fig. 1. Cell configuration for testing the photocatalytic efficiency of the titania membrane. (a) Diffusion cell; (b) Permeation cell.

From such formulated sol and usual deposition procedures, it is possible to easily reproduce homogenous and defect-free membranes with a thickness of ~3 μm (Fig. 2). Such thickness is convenient to overcome possible large defects on the substrate surface. Moreover no significant infiltration can be detected in the alumina support (Fig. 2).

From the N_2 adsorption–desorption isotherm of powder B, it can be deduced that the specific surface area, S_{BET} is equal to 190 $m^2\ g^{-1}$ and that the material is mesoporous with a mean pore size equal to 12 nm and a porosity of 68%. The measured mean pore size is in agreement with packing of 30–60 nm sized particles. As expected, this range of pores corresponds to that of an ultrafiltration membrane.

3.2. Membrane properties

The linear evolution of pure water flow versus transmembrane pressure is shown in Fig. 3a. The water permeance is determined from the slope. It is equal to ~150 $L\,h^{-1}\,m^{-2}\,bar^{-1}$ and more than one order of magnitude lower than that of the tubular support alone (~1800 $L\,h^{-1}\,m^{-2}\,bar^{-1}$). The intrinsic membrane permeability B_0 was determined from these data applying the Darcy's law. Assuming a linear transmembrane pressure gradient located in the separative layer, the expression of the measured membrane permeability, B_{0mes}, is:

$$B_{0mes} = \frac{J\eta_L e}{\Delta P}$$

with J, the measured flux of water; η_L, the dynamic viscosity of water; e, the membrane thickness; ΔP, the transmembrane pressure.

The determined value for B_{0mes} is 9×10^{-19} m^2. The same order of magnitude, i.e. 2×10^{-19} m^2, is obtained for the calculated value, B_{0cal}, determined from the porous characteristics measured with powder B and using the Carman–Kozeny equation [24]:

$$B_{0cal} = \frac{\varepsilon^3}{5[(1-\varepsilon) \times S_{BET} \times \rho_D]^2}$$

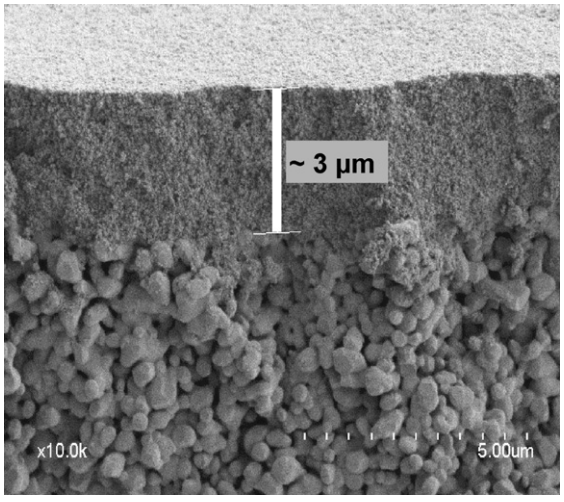

Fig. 2. SEM cross-section image of the titania layer deposited on the tubular macroporous alumina support.

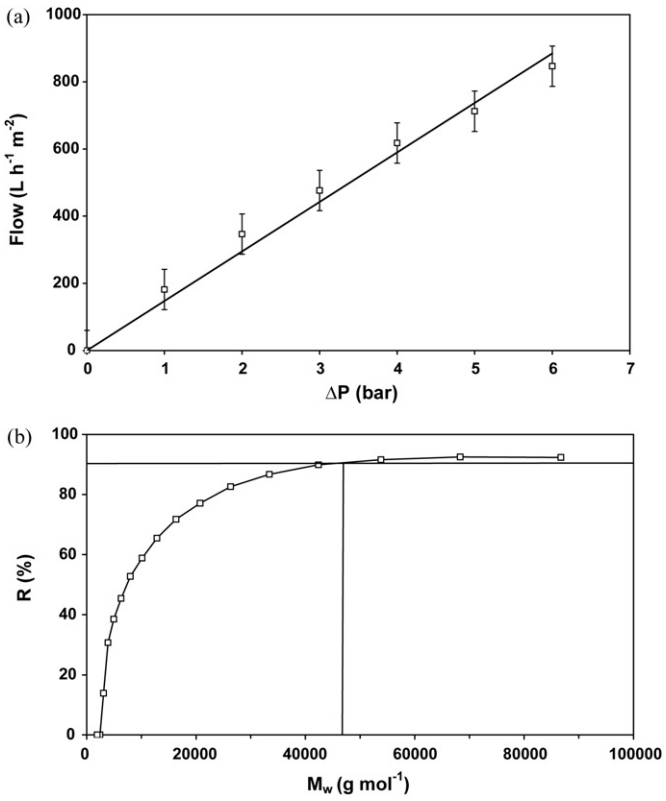

Fig. 3. (a) Water flow versus transmembrane pressure; (b) Rejection rate versus solute molecular weight.

with ε, the porosity, and ρ_D, the skeletal density of the layer, i.e., the density of anatase.

As previously mentioned, the measured specific surface area used in the Carman–Kozeny equation overestimated the value of the specific surface area developed by the intergranular porosity which is not involved in the transport across the membrane. As a consequence, the calculated value for the membrane permeability is underestimated. On the other hand, the rather good agreement between calculated and measured values of permeability confirms the limited infiltration of the titania sol in the support. The membrane thickness estimated by SEM corresponds to the effective thickness of the membrane.

Retention data were collected from permeation experiments using an aqueous solution containing a mixture of Dextran® as feed. The membrane molecular weight cut-off (MWCO) was determined from the retention curve (Fig. 3b). Although the curve does not exactly reach 100% for the largest molecular weights (probably due to membrane fault sealing), MWCO can be estimated at ~50 kDa. This value is in agreement with the mean pore size previously measured with powder B.

3.3. Photocatalytic properties

In order to enable the comparison of the photocatalytic performance of material B with a reference photocatalyst like powder P25, experiments were first performed with powders. The photocatalytic efficiency of powder B was initially evaluated from the methylene blue photodegradation experiments. Its efficiency is rather good although it is lower than that of the reference powder P25 (Fig. 4a). These curves fit rather well with the kinetic model of Langmuir–Hinshelwood usually adapted for cases of low concentrations of organic solute [25].

Equivalent experiments performed with phenol led to quite different results (Fig. 4b and c). A measurable photocatalytic effect is evidenced (Fig. 4b) but, in this case, the performance of powder B is very low compared to that of powder P25 (Fig. 4c). It is well known that the photocatalytic process is complex and very sensitive to the nature of the organic molecule to be photo-oxidized and also to the crystalline state of the titania powder [16–19]. On the other hand, it must be underlined that even after grinding, equivalent powder B consists in larger aggregates than powder P25. As a consequence the accessibility to the photocatalytically active titania surface is lower for powder B. This is unfavorable for reactant transport towards the active sites and for desorption and extraction of photodegradation products.

Investigations were then performed on membranes with diffusion experiments of organics across a titania layer deposited on a porous alumina disk. The evolution versus time of the concentration of MB in the reception tank is illustrated with Fig. 5a and b. Different equivalent experiments were performed in order to check the reproducibility. Even if the curves are not exactly the same, the same trends are observed.

During the irradiation times, a decrease of MB concentration is observed in the reception tank. In some cases, the final concentration at the end of the irradiation period is lower than the initial concentration at the beginning of the previous period with UV. This result indicates that the destroyed amount of MB is larger than that crossing the membrane by diffusion. The layer works also as a classical photoreactor with photocatalyst immobilized on the reactor wall.

Except the periods of alternated UV irradiation, the evolution versus time of MB concentration in the reception tank increases in agreement with Fick diffusion regime as previously observed [9]. Moreover, thanks to the initial saturation of the membrane surface, the mass balance in solution (feed and reception) is correctly respected.

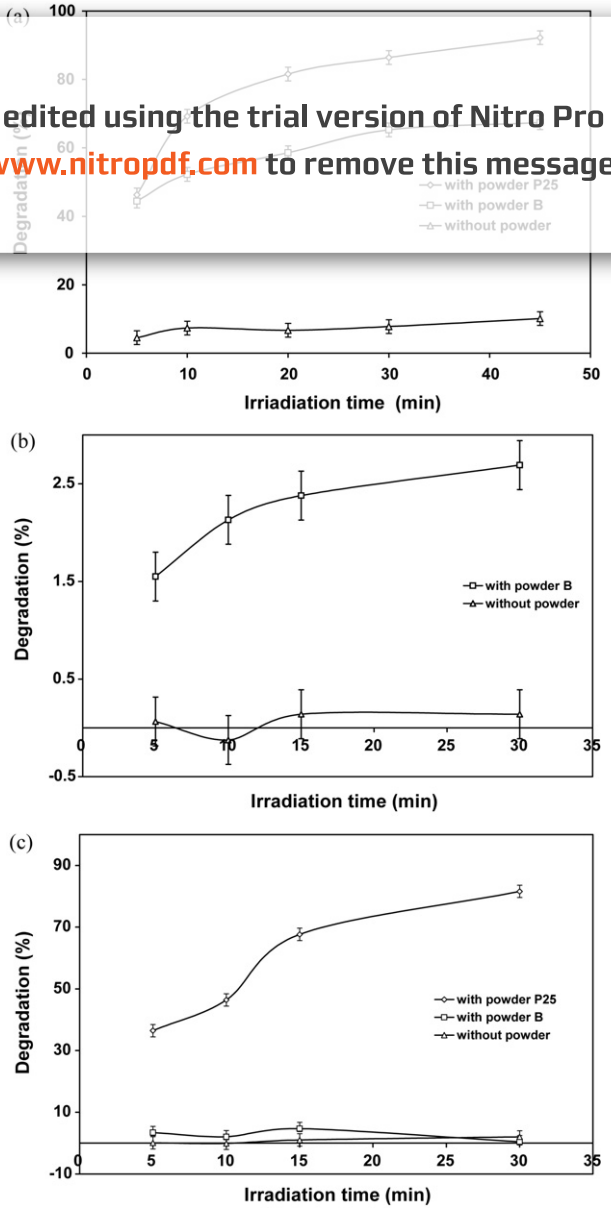

Fig. 4. UV photodegradation experiments with powders. (a) MB photodegradation with $[MB]_0 = 1.5 \times 10^{-5}$ mol L^{-1}; (b) phenol photodegradation with $[phenol]_0 = 10^{-3}$ mol L^{-1}; (c) phenol photodegradation with $[phenol]_0 = 10^{-4}$ mol L^{-1}.

From the change of slope corresponding to the UV irradiation periods, it is possible to evaluate δ, the quantity of destroyed MB per units of time and of membrane surface area (Fig. 6). Due to the low evolution of solute concentration in the reception tank during short periods of few hours, the applied linear interpolation and extrapolation are clearly acceptable. δ is equal to $\sim 0.8 \times 10^{-8}$ mol s^{-1} m^{-2} during the first hours of the experiment and reaches $\sim 2.3 \times 10^{-8}$ mol s^{-1} m^{-2} after few tens of hours. This last value is around on fifth of that previously measured with an alumina microfiltration membrane whose grains were coated with a highly photoactive mesostructured titania coating: $0.9–1.0 \times 10^{-7}$ mol s^{-1} m^{-2} [9]. On the other hand, it is more than one order of magnitude larger than the value measured for a ZnO-based UF membrane: 1.5×10^{-9} mol s^{-1} m^{-2} [26]. When MB is replaced by phenol (Fig. 5c), the quantity of destroyed

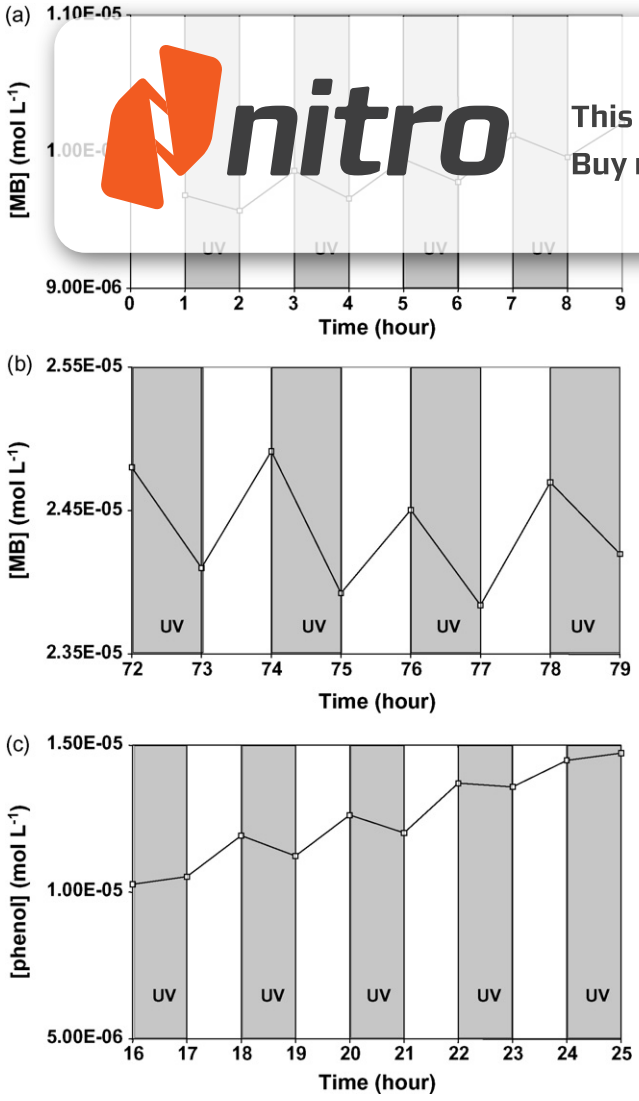

Fig. 5. UV photodegradation experiments with a titania membrane in a diffusion cell: evolution versus time and UV irradiation of the organic molecule concentration in the reception tank (a) and (b) initial concentration of MB in the feed tank = 10^{-4} mol L^{-1}; (c) initial concentration of phenol in the feed tank = 10^{-3} mol L^{-1}.

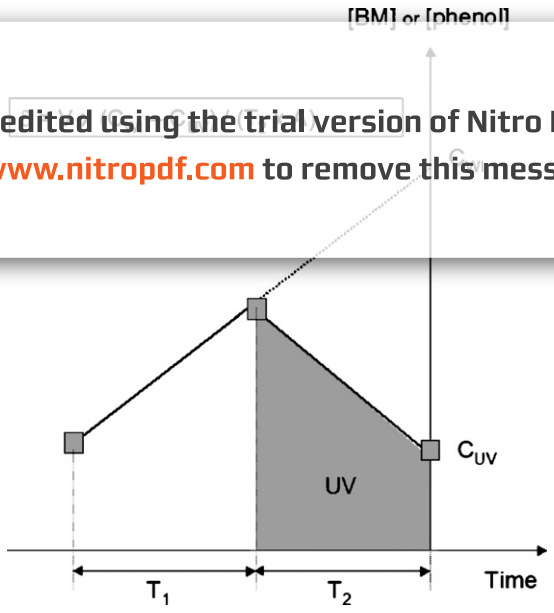

Fig. 6. Method used for the calculation of δ, quantity of destroyed organic solute per units of time and of membrane surface area. C_{UV} is the concentration of organic solute measured in the reception tank at the end of an UV irradiation period. C_{WI} is the concentration of organic solute which should be observed in absence of UV irradiation. It is roughly estimated from the linear extrapolation of the concentration increase during the previous period, T_1, without UV irradiation. V is the volume of liquid in the reception tank. T_2 is the duration of the UV irradiation period. A is the membrane area. In our case, $T_1 = T_2 = 1$ h.

solute per units of time and of membrane surface area, progressively decreases during the first hours of the experiment ($\sim 3.8 \times 10^{-8}$ mol s^{-1} m^{-2} at $t = 18$ h and $\sim 1.1 \times 10^{-8}$ mol s^{-1} m^{-2} at $t = 24$ h). This decrease of activity can be explained by the formation of various products of phenol photo-oxidation [27,28] which would be progressively adsorbed on the titania surface and would hinder the access for new phenol molecules.

The parameter δ can usefully be applied to evaluate the membrane applicability taking into account the pollutant content in the water to be treated and to scale-up of the purification unit. Using the value of δ measured for MB and the water permeation data measured with tubular membranes (Fig. 3a), dynamic measurements (Fig. 1b) were performed with an aqueous solution of MB with a concentration of 2×10^{-7} mol L^{-1} and with a transmembrane pressure ΔP equal to 1.2 bar. It was expected than all the

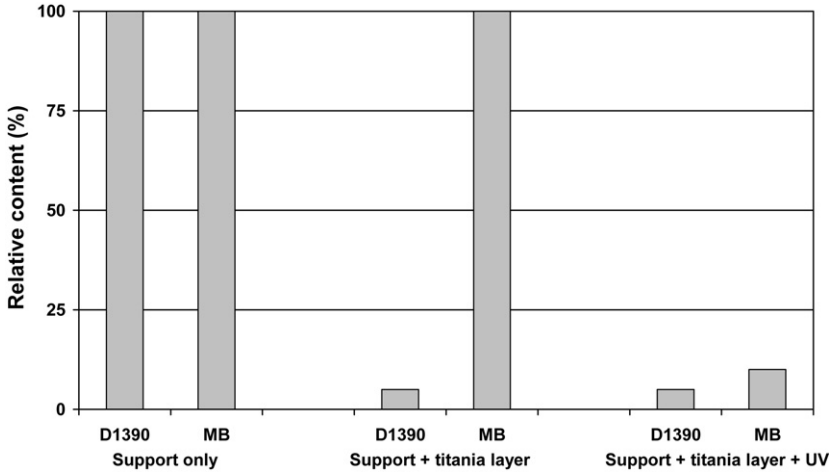

Fig. 7. Summary of the results obtained by testing the separation and photocatalytic performance in dynamic conditions. The relative content corresponds to the ratio of the solute concentration measured in the permeate to the solute concentration in the feed solution.

MB molecules crossing should be degraded at the membrane surface. The chemical analysis of the permeate showed that only 10% of the MB content of the feed remained in the permeate. This result is rather good taking into account the accuracy of the estimation for δ and the possible presence of membrane and/or sealing defects. Fig. 7 summarizes the results obtained for the separation and photocatalytic performance in dynamic conditions and illustrates the potentialities of this membrane.

4. Conclusion

A simple and robust synthesis route has been developed to prepare a photocatalically active titania-based ultrafiltration membrane from a commercial titania hydrosol and alumina supports. The membrane performance in term of separation and photocatalytic activity has been measured. The photocatalytic efficiency is better for the reference organic dye (methylene blue) than for phenol selected as typical organic pollutant in water.

Membrane calcination at higher temperature (550–650 °C) will be tested in order to induce a partial structural transition of anatase into rutile. It is expected to improve the photocatalaytic efficiency taking into account the better efficiency observed with the reference powder P25. As a counterpart, it will result into microstructure modification and related change in separative properties that will be also investigated. The identification of the different products resulting from the photodegradation of organic solutes will also be considered.

In parallel, a filtration pilot enabling coupled membrane separation and photcatalytic degradation in dynamic conditions for different transmembrane pressures will be built in order to test possible technological applications of such device with water solutions containing different types of organic solutes which are present in industrial or public waste waters.

Acknowledgements

The authors thank D. Cot and V. Bonniol (IEM, Montpellier, France) for their help with characterization. Financial support from the Algerian Ministry of Higher Education and Scientific Research and the French Ministry of Foreign Affairs in the scope of the bilateral French–Algerian TASSILI project no. 09mdu763 is gratefully acknowledged.

References

[1] J. Mo, Y. Zhang, Q. Xu, J. Joaquin Lamson, R. Zhao, Photocatalytic purification of volatile organic compounds in indoor air: a literature review, Atmospheric Environ. 43 (2009) 2229–2246.
[2] J.M. Herrmann, Heterogeneous photocatalysis: fundamentals and applications to the removal of various types of aqueous pollutants, Catal. Today 53 (1999) 115–129.
[3] R. Molinari, L. Palmisano, E. Drioli, M. Schiavello, Studies on various reactor configurations for coupling photocatalysis and membrane processes in water purification, J. Membr. Sci. 206 (2002) 399–415.
[4] R. Molinari, M. Borgese, F. Drioli, L. Palmisano, M. Schiavello, Hybrid processes coupling photocatalysis and membranes for degradation of organic pollutants in water, Catal. Today 75 (2002) 77–85.
[5] D.F. Ollis, Integrating photocatalysis and membrane technologies for water treatment, Ann. N. Y. Acad. Sci. 984 (2003) 65–84.
[6] R. Molinari, F. Pirillo, V. Loddo, L. Palmisano, Heterogeneous photocatalytic reactors on photodegradation of Acid Yellow 36 in a hybrid photocatalysis–membrane
[7] T. Tsuru, T. Toyosada, T. Yoshioka, M. Asaeda, Photocatalytic reactions in a filtration system through porous titanium dioxide membranes, J. Chem. Eng. Jpn. 34 (2001) 844–847.
[8] T. Tsuru, T. Kan-no, T. Yoshioka, M. Asaeda, A photocatalytic membrane reactor for gas-phase reactions using porous titanium oxide membranes, Catal. Today 82 (2003) 41–48.
[9] F. Bosc, A. Ayral, C. Guizard, Mesoporous anatase coatings for coupling membrane separation and photocatalyzed reactions, J. Membr. Sci. 265 (2005) 13–19.
[10] H. Choi, E. Stathatos, D.D. Dionysiou, Sol–gel preparation of mesoporous photocatalytic TiO_2 films and TiO_2/Al_2O_3 composite membranes for environmental applications, Appl. Catal. B: Environ. 63 (2006) 60–67.
[11] H. Choi, E. Stathatos, D.D. Dionysiou, Photocatalytic TiO_2 films and membranes for the development of efficient wastewater treatment and reuse systems, Desalination 202 (2007) 199–206.
[12] A. Fujishima, K. Hashimoto, T. Watanabe, TiO_2 Photocatalysis, Fundamentals and Applications, BKC Inc., Tokyo, 2001.
[13] K. Rajeshwar, Photoelectrochemistry and the environment, J. Appl. Electrochem. 25 (1995) 1067–1082.
[14] K.M. Schindler, M. Kunst, Charge carrier dynamics in TiO_2 powders, J. Phys. Chem. 94 (1990) 8222–8226.
[15] Y.H. Hsien, C.F. Chang, Y.H. Chen, S. Cheng, Photodegradation of aromatic pollutants in water over TiO_2 supported on molecular sieves, Appl. Catal. 31 (2001) 241–249.
[16] S. Cheng, S.-J. Tsai, Y.-F. Lee, Photocatalytic decomposition of phenol over titanium oxide of various structures, Catal. Today 26 (1995) 87–96.
[17] T. Ohno, K. Sarukawa, K. Tokieda, M. Matsumura, Morphology of a TiO_2 photocatalyst (Degussa, P-25) consisting of anatase and rutile crystalline phases, J. Catal. 203 (2001) 82–86.
[18] B. Sun, P.G. Smirniotis, Interaction of anatase and rutile TiO_2 particles in aqueous photooxidation, Catal. Today 88 (2003) 49–59.
[19] J. Medina-Valtierra, J. Garcıa-Servın, C. Frausto-Reyes, S. Calixto, The photocatalytic application and regeneration of anatase thin films with embedded commercial TiO_2 particles deposited on glass microrods, Appl. Surf. Sci. 252 (2006) 3600–3608.
[20] F. Bosc, Synthèse et caractérisation de couches minces et de membranes photocatalytiques à base de TiO_2 anatase, PhD Thesis, University Montpellier 2, France, 2004.
[21] N. Veronovski, P. Andreozzi, C. La Mesa, M. Sfiligoj-Smole, Stable TiO_2 dispersions for nanocoating preparation, Surf. Coat. Technol., in press, doi:10.1016/j.surfcoat.2009.09.041.
[22] E.P. Barrett, L.G. Joyner, P.P. Halenda, The determination of pore volume and area distributions in porous substances. I. Computations from nitrogen isotherms, J. Am. Chem. Soc. 73 (1951) 373–380.
[23] S. Brunauer, P.H. Emmet, E. Teller, Adsorption of gases in multimolecular layers, J. Am. Chem. Soc. 60 (1938) 309–319.
[24] C.J. Brinker, G.W. Scherer, Sol–Gel Science, the Physics and Chemistry of Sol–Gel Processing, Academic Press, N.Y., 1990.
[25] J. Cunningham, G. Al-Sayyed, P. Sedlak, J. Caffrey, Aerobic and anaerobic TiO_2-photocatalysed purifications of waters containing organic pollutants, Catal. Today 53 (1999) 145–158.
[26] L. Naszalyi, F. Bosc, A. El Mansouri, A. van der Lee, D. Cot, Z. Horvolgyi, A. Ayral, Sol–gel-derived mesoporous SiO_2/ZnO active coating and development of multifunctional ceramic membranes, Sep. Purif. Technol. 59 (2008) 304–309.
[27] R. Alnaizy, A. Akgerman, Advanced oxidation of phenolic compounds, Adv. Environ. Res. 4 (2000) 233–244.
[28] S.G. Poulopoulos, F. Arvanitakis, C.J. Philippopoulos, Photochemical treatment of phenol aqueous solutions using ultraviolet radiation and hydrogen peroxide, J. Hazard. Mater. B129 (2006) 64–68.